SPACECRAFT ALIGNMENT DETERMINATION AND CONTROL FOR DUAL SPACECRAFT PRECISION FORMATION FLYING

Philip C. Calhoun,* Anne-Marie Novo-Gradac,† and Neerav Shah‡

Many proposed formation flying missions seek to advance the state of the art in spacecraft science imaging by utilizing dual-spacecraft precision formation flying (PFF) to enable a "virtual" telescope (VT). Using precision dual-spacecraft alignment, very long focal lengths can be achieved by locating the optics on one spacecraft and the detector on the other. Proposed science missions include astrophysics concepts for X-ray imaging and exo-planet observation with large spacecraft separations (1000 km to 80,000 km), and heliophysics concepts for X-ray or extreme ultra-violet (EUV) imaging or solar coronagraphs with smaller separations (50m – 500m). These proposed missions require advances in guidance, navigation, and control (GN&C) for PFF to enable high resolution science imaging. For many applications, the dual-spacecraft dynamics are coupled through the GN&C system when the relative ranging and position alignment sensor components are not co-located with their respective spacecraft mass centers. We develop a model-based PFF system design approach for the VT application, considering the coupling inherent in precision dual-spacecraft inertial alignment. These systems employ a variety of GN&C sensors and actuators, including laser-based alignment and ranging systems, camera-based imaging sensors, inertial measurement units (IMU), as well as microthruster systems and image motion compensation platforms. Results of a GN&C performance assessment reveal how data from relative position sensors can be employed in a Kalman filter framework to significantly improve alignment estimation performance. The assessment provides a comparison of two different GN&C formation flying architectures, illustrating the performance trades inherent in the choice of PFF system architecture in the VT application.

INTRODUCTION

Many proposed formation flying missions seek to advance the state of the art in spacecraft science imaging by utilizing dual-spacecraft precision formation flying (PFF) to enable a "virtual" telescope. The virtual telescope (VT) is formed by inertial alignment of an Optics (or Occulter) spacecraft relative to a Detector spacecraft at a nominally fixed separation, depending on the telescope focal length. A functioning telescope with very long focal lengths can be achieved in this manner using precision dual-spacecraft alignment. Proposed VT science missions include astrophysics investigations using formation flying spacecraft with separations from 1000 km to 80,000 km, such as the Milli-Arc-Second Structure Imager (MASSIM)[1,2] the New Worlds Observer

* Senior Aerospace Engineer, Attitude Control System Engineering Branch, NASA Goddard Space Flight Center, Mail Stop 591, 8800 Greenbelt Rd. Greenbelt, Md. 20771.
† Senior Aerospace Engineer, Heliophysics Laboratory, NASA Goddard Space Flight Center, Mail Stop 672, 8800 Greenbelt Rd., Greenbelt, Md. 20771.
‡ Associate Branch Head, Navigation and Orbit Design Branch, NASA Goddard Space Flight Center, Mail Stop 595, 8800 Greenbelt Rd. Greenbelt, Md. 20771.

(NWO)[3,4,5,6], heliophysics concepts for solar coronagraphs[7,8], and x-ray imaging[9] with smaller separations (50m – 500m). These proposed missions require advances in PFF of two spacecraft. In particular, very precise inertial alignment control and estimation is required for inertial pointing of the "virtual" telescope to enable high resolution science imaging (e.g. milli-arc-sec). Figure 1 shows the dual-spacecraft inertial (i.e. astrometric) alignment VT concept for a leader/follower formation flying architecture. A single optical sensor mounted on the Follower spacecraft is used to track the Leader spacecraft relative to an inertial guide star target within the sensor field of view.

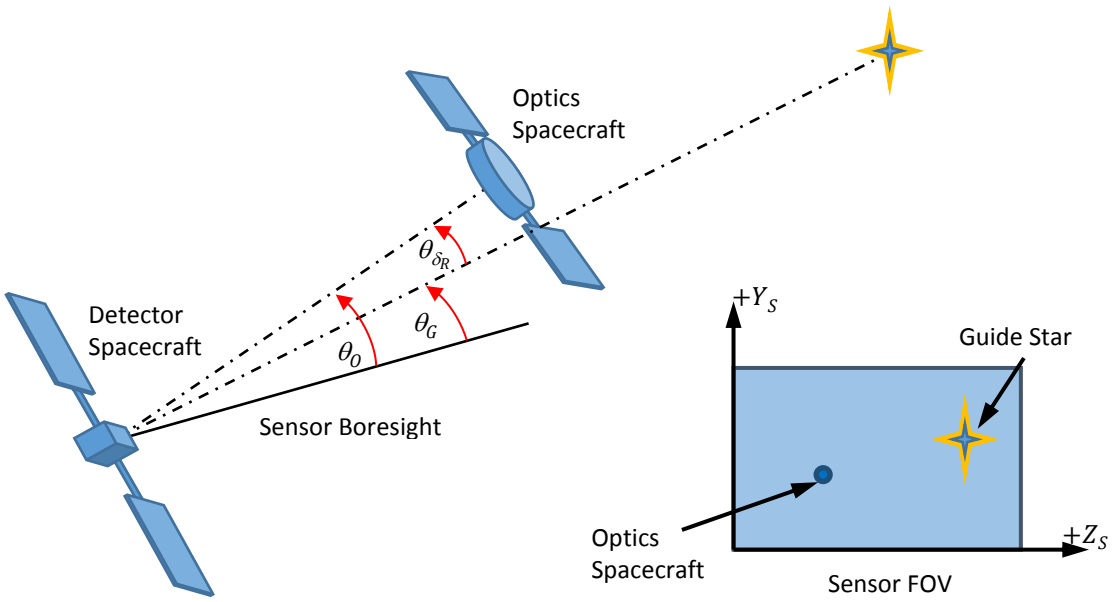

Figure 1. Dual-Spacecraft Precision Inertial Alignment Sensing Concept.

We develop the dynamics, sensor models, and GN&C architectures necessary to implement onboard systems for PPF of this dual-spacecraft VT concept. These systems employ a variety of GN&C sensors and actuators, including laser-based alignment and ranging systems, optical relative navigation sensors, star trackers, inertial measurement units (IMU), as well as microthruster and precision stabilized image motion compensation systems. For many applications, the use of relative ranging and position alignment sensors results in kinematic coupling of the two spacecraft through the GN&C system when sensor components are not co-located with the respective spacecraft mass centers. While this adds complexity to the typical telescope pointing design, it also provides the GN&C engineer with an opportunity to exploit this coupling through the use of model based methods.

Previous work included a consider-state analysis method for evaluation of dual-spacecraft relative navigation and architectures for precise inertial alignment[5]. That work focused on transverse alignment only because those degrees of freedom are the most critical for VT precision GN&C, particularly for the longer baseline missions such as MASSIM[1] and NWO[2]. We extend the analysis to include all translational and rotational degrees of freedom for a more generic VT specification including attitude and range states. While this full-state model-based framework is generally applicable over a wide range of spacecraft separations (including for long baseline astrophysics missions), it is particularly important for PFF in shorter baseline operation (50-500m) where attitude coupling is significant, such as for several proposed heliophysics missions. A systematic method for relating the basic VT science instrument specifications for image smear and depth of focus to the attitude and translational requirements is provided in this work. This method is then used to develop models for the relative position and alignment measurements from optical sensors to be used in the GN&C framework for control design.

We include a summary of a complete dynamics and control model framework for the development of alignment estimation and control algorithms. The basic equations for relative flight dynamics of two spacecraft flying in precise formation are developed by numerous authors, as summarized by Calhoun[10]. We use Luquette's formulation[11-14] of the relevant dynamics in an inertial reference as a basis for the GN&C design and analysis. A summary of relevant inertial sensor component models is also included in this paper. The models developed herein form a framework for full-state alignment filter and control system design methods. An example GN&C design for a proposed heliophysics VT mission concept is provided as a case study. The study results illustrate how a Kalman filter framework can be employed to significantly reduce the alignment error over that obtained from the baseline measurements. The case study also provides a comparison of two different GN&C formation flying architectures, illustrating the performance trades inherent in PFF for the VT application.

VT STABILITY REQUIREMENTS AND MEASUREMENT MODELS

Optical metering structures for large monolithic space telescopes are necessary for precise optics to detector alignment stability. However, they are impractical for on-orbit applications with long baselines (e.g. focal length > 50m). Launch vehicle payload constraints would require large and complex metering structures, deployed or assembled on-orbit. PFF of separate free-flying platforms for optics and detector assemblies may be used to "replace" the optical metering structure. The GN&C system provides a stable alignment for these assemblies, establishing a "virtual" platform for telescope pointing and stability. This type of PFF places unique requirements on the separated optics and detector platform dynamics and control, involving nine degrees of freedom (DoF) to fully characterize the image smear and stability of the depth of focus. The formation flying GN&C approach for dual-spacecraft rendezvous, proximity operation, or constellation management, involves at most the relative six DoF between platforms. The inertial alignment of the two free flying vehicles is usually not relevant. In this section, we develop the equations for the VT science imaging smear and depth of focus as a function of the nine DoF inherent in dual-spacecraft inertial alignment. This method is also applied to the development of measurement models for optical alignment and ranging sensor systems.

Attitude and Translation Stability Requirements

The first step in the GN&C design and analysis of the VT PFF systems and architectures is to derive requirements for the six attitude and three translational DoF for the dual-spacecraft formation as a function of the science imaging requirements at the detector. The following development is a formalization of the method provided by Novo-Gradac[15]. Figure 2 shows a breakdown of attitude and translational displacements starting from an ideal VT alignment of the detector and optics assemblies (i.e. no rotational or translational deviations from ideal optical axes), which is shown in blue. The green frame represents translational displacement of the optics assembly off the line-of-sight from detector to target. The red frame represents rotational motion for both Optics spacecraft and Detector spacecraft. The resulting shift in optics center of focus from detector center is shown in Figure 2. From inspection of Figure 2 it can be deduced that the image stability, $\vec{\delta}_I$, with components image smear, s_x , s_y , and depth of focus, d_z, is expressed in terms of the spacecraft relative translational DoF, $\vec{\delta}_R$, and absolute rotational DoF for Detector spacecraft, $\vec{\theta}_D$, and Optics spacecraft, $\vec{\theta}_O$, as,

$$\vec{\delta}_I = \begin{bmatrix} s_x \\ s_y \\ d_z \end{bmatrix} = \left[\vec{P}_D + \vec{P}_{DO} + \vec{\delta}_R - \vec{P}_O + R(\vec{\theta}_O)\vec{P}_O + f\left(R(\vec{\theta}_O)\right)\vec{P}_{OD}\right] - R(\vec{\theta}_D)\vec{P}_D . \quad (1)$$

Where the rotational operators, $R(\vec{\theta})$, can be expressed in terms of a small angles, $\vec{\theta}$, using cross

product operator notation, $\tilde{\theta}$,

$$R(\vec{\theta}) = [\, I + \tilde{\theta}\,]\,. \tag{2}$$

The function *f* is a mapping of focal plane image distortion (i.e. smear and depth of field) due to small rotations of the Optics assembly. This effect on VT center of focus is illustrated in Figure 2 by slight rotation of the optical imaging due to the Optics spacecraft rotation. This would in general be non-linear and dependent on the optics design, but could be linearized for small angles, as

$$f\left(R(\vec{\theta}_O)\right) = [I] + {}^n\vec{\theta}_O\,, \qquad {}^n\vec{\theta}_O = \Phi\,\vec{\theta}_O\,. \tag{3}$$

Where the elements of Φ, ϕ_{ij}, are scaling factors ($0 < \phi_{ij} < 1$) derived from the optics design. These factors would be negligible (i.e. $\phi_{ij} \sim= 0$) for small angular displacements of a diffractive optics assembly used in many x-Ray and extreme ultra-violet (EUV) VT applications. Combining (2) and (3) into (1) provides a simplified representation that serves as a basis for error analysis of image distortion in terms of requirements for the attitude and translation DoF.

$$\vec{\delta}_I = \begin{bmatrix} s_x \\ s_y \\ d_z \end{bmatrix} = \tilde{P}_D\,\vec{\theta}_D + [\Phi\,\tilde{P}_{DO} - \tilde{P}_O\,]\vec{\theta}_O + \vec{\delta}_R\,. \tag{4}$$

Equation 4 represents the coupling of the attitude and translational DoF for science imaging when the separated detector and optics components are not co-located with their respective spacecraft mass centers.

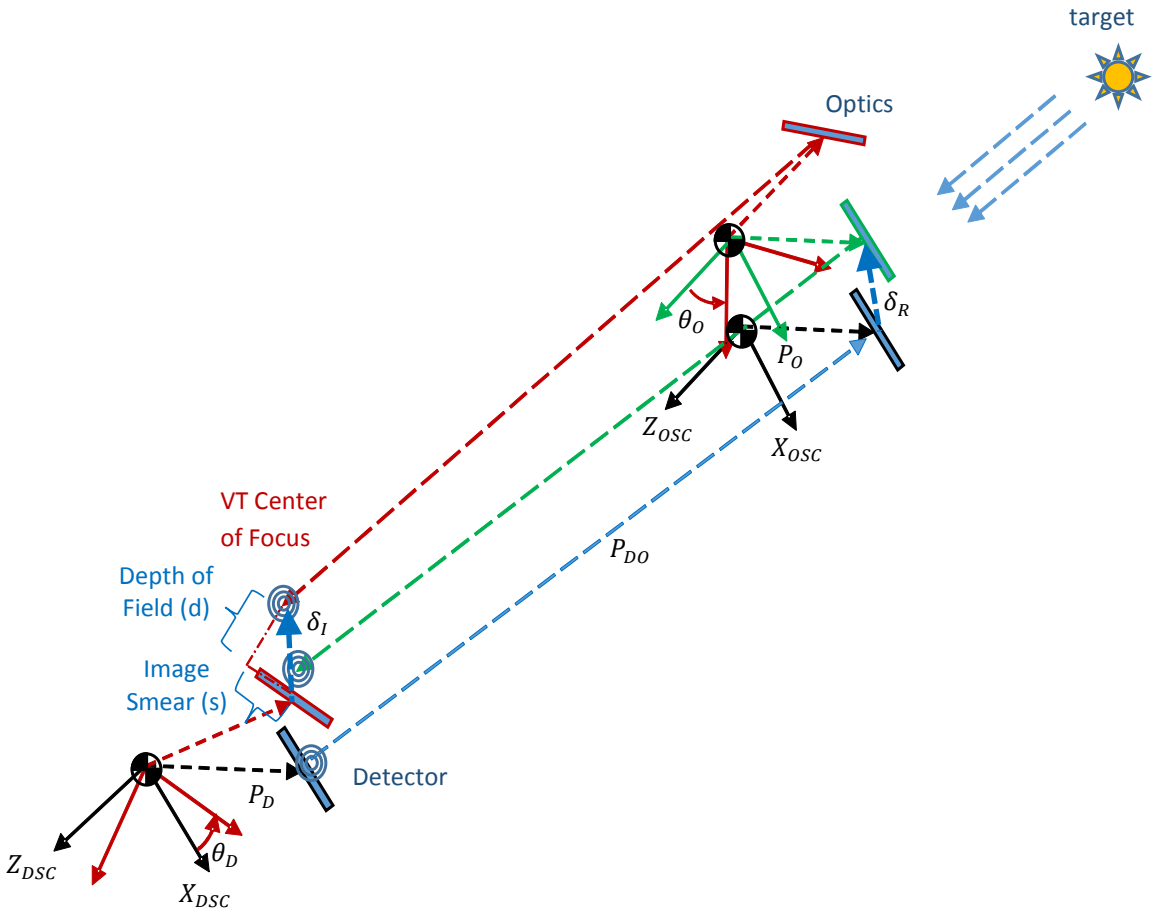

Figure 2. Detector Image Smear and Depth of Focus as function of Attitude and Translation.

Optical Alignment and Ranging System Measurement Models

The method given in the previous section to develop the science imaging requirements can also be used to model the relative position measurement for various optical (i.e. laser and camera) alignment and ranging components, illustrating this same 9 DoF coupling in the GN&C system design.

The laser alignment system utilizes a position sensing detector mounted on the Detector spacecraft to measure the lateral alignment offset of an illuminated spot from a collimated laser source mounted on Optics spacecraft[16]. A non-collocated laser ranging system is also used to precisely measure the relative range. Then we can use Eq. (4) as a laser alignment and ranging measurement model by replacing appropriate variables,

$$\vec{\delta}_L = \begin{bmatrix} l_x \\ l_y \\ r_z \end{bmatrix} = \tilde{P}_L \vec{\theta}_D + [\Phi \tilde{P}_{LB} - \tilde{P}_B]\vec{\theta}_O + \vec{\delta}_R . \quad (5)$$

Where $\vec{\delta}_L$ represents the measured displacements from laser spot detector center, in terms of alignment errors, l_x, l_y, and ranging errors, r_z. The variables, $\tilde{P}_L, \tilde{P}_B, \tilde{P}_{LB}$, represent the cross product operators for position vectors of the laser detector elements on the Detector spacecraft, the laser beacon elements on Optics spacecraft, and the relative position from laser detectors to beacons, respectively. For this model, the scaling matrix diagonal elements, ϕ_{ii}, are set equal to 1 for a laser beacon mounted on the Optics spacecraft. They are set equal to 0 if the beacon is collocated with the detector and a corner cube reflector, mounted on Optics spacecraft, serves as the virtual beacon.

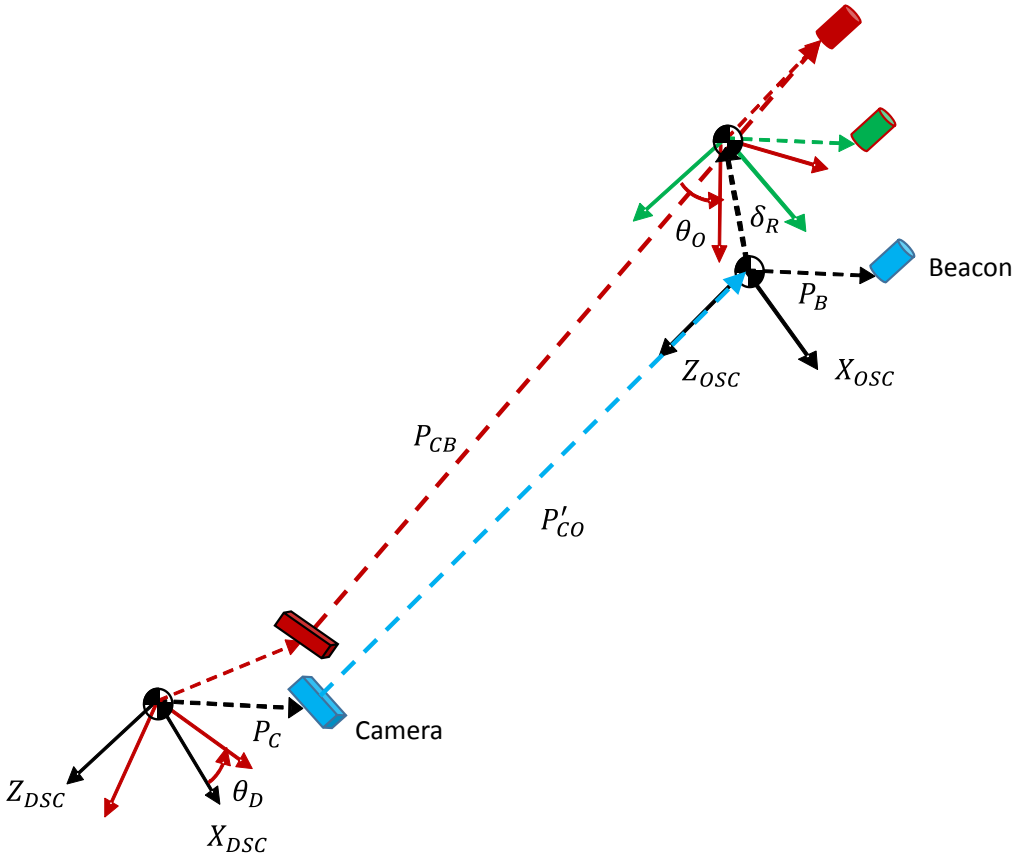

Figure 3. Alignment Camera line-of-sight as function of Attitude and Translation.

An alignment camera (e.g. similar to the Advanced Video Guidance Sensor (AVGS)[17,18]) mounted on the Detector spacecraft can be also be used to measure the relative spacecraft alignment by tracking laser beacons or retro reflectors mounted on the Optics spacecraft. The measurement model for this camera-based sensor can be derived as follows. From inspection of Figure 3 it is deduced that the location of a tracked laser beacon on Optics spacecraft, relative to the alignment camera image plane center, $\vec{P}_{CB}$, is expressed in terms of the spacecraft relative translational $\vec{\delta}_R$, and absolute rotational, $\vec{\theta}_D, \vec{\theta}_O$ DoF as,

$$\vec{P}_{CB} = \left[\vec{P}_C + \vec{P}_{CO} + \vec{\delta}_R + R(\vec{\theta}_O)\vec{P}_B \right] - R(\vec{\theta}_D)\vec{P}_C \,. \tag{6}$$

Then, the laser beacon spot centroid on the camera image can be expressed in terms of angles, θ_x, θ_y.

$$[\theta_x, \theta_y] = \left[\text{atan}\left(\frac{\vec{P}_{CB}(2)}{\vec{P}_{CB}(3)}\right), \text{atan}\left(\frac{\vec{P}_{CB}(1)}{\vec{P}_{CB}(3)}\right) \right]. \tag{7}$$

VT DYNAMICS AND CONTROLS FRAMEWORK FOR GN&C DESIGN

A complete framework for the VT GN&C system design for PFF combines system dynamics and inertial sensor models with the optical sensor measurement models given in the previous section. In this section we provide a summary of the dynamics and inertial sensor models presented in prior work by Calhoun[10]. Two possible GN&C architectures are also presented to illustrate and compare practical solutions for PFF.

Dynamics Model Formulation and Inertial Measurement Models

The relative flight dynamics of two spacecraft in formation has been previously studied by numerous authors with applications to formation flying technology development, as summarized by Calhoun[10]. These generally fit into two categories. The formation dynamics in a close orbit to a single gravitational body (e.g. low Earth orbit) and deep space applications. We use Luquette's formulation[6-14] of the relevant dynamics in an inertial reference as a basis for the GN&C design and analysis since many VT missions are in deep space applications. The dynamic equations of motion in a simplified form for the Optics spacecraft with respect to the Detector spacecraft, given herein, are a summary of the results from Calhoun.[10] They include modifications to Luquette's formulation to include additional gravitational bodies and to develop the equation parameters in terms of the Detector (Follower) spacecraft reference. This provides for ease of implementation in an autonomous leader/follower formation architecture with the Detector spacecraft serving as the follower. The dynamics model also includes three-axis attitude dynamics for both Optics spacecraft and Detector spacecraft.

The translational dynamics of relative motion can be expressed in term of the relative position of Detector spacecraft with respect to the Optics spacecraft (Note: [I] represents the 3x3 identity matrix).[5]

$$\ddot{\vec{x}} = -\sum_{i=1}^{n} \frac{\mu_i}{\|\vec{r}_{iD}\|^3} \left([I] - 3\vec{r}_{iD}\vec{r}_{iD}{}^T \right) \vec{x} + \Delta\vec{f}_{solar} + \Delta\vec{f}_{pert} + \vec{u}_{thrust,D} - \vec{u}_{thrust,O} \tag{8}$$

Since these equations of motion for dual-spacecraft relative dynamics are developed in a general linear parametric form, they are suitable for design and evaluation of VT GN&C systems in a variety of applications. This model can be applied to control and estimation during all phases of a typical dual-spacecraft formation flying mission, including formation reorientation, initial formation alignment acquisition, and precision alignment operations. Formation flying for the VT in a leader/follower architecture is facilitated by using this form of the relative dynamics, since 1) the equations are expressed in an inertial reference frame and 2) the gravitational body ephemeris data are expressed relative to the Detector spacecraft (follower) reference.

A linear time-invariant (LTI) form of Eq. (8), is formulated by expressing the relative position state, $\vec{x}$, in terms of a perturbed range state, $\vec{\delta}_R$, and a nominal reference range, $\vec{R}^{ref}$, between the two spacecraft for the virtual telescope configuration.

$$\vec{x} = \vec{R}^{ref} + \vec{\delta}_R \tag{9}$$

$$\ddot{\vec{\delta}}_R = \Gamma_{GG}\,\vec{\delta}_R + \Gamma_{GG}\,\vec{R}^{ref} + \vec{u}_R \tag{10}$$

A gravity gradient parameter matrix, Γ_{GG}, is expressed in terms of fixed parameters referenced to the Detector spacecraft.

$$\Gamma_{GG} = -\sum_{i=1}^{n} \frac{\mu_i}{\left\|\vec{r}_{iD}{}^{ref}\right\|^3}\left([I] - 3\hat{r}_{iD}{}^{ref}\left[\hat{r}_{iD}{}^{ref}\right]^T\right) \tag{11}$$

Eq. (10) and Eq. (11) then form a LTI dynamics model. They represent the relative dynamics of dual-spacecraft formation when considering small displacements from a fixed relative reference trajectory. Approximations used to arrive at this final linear form are particularly applicable to a tightly-controlled inertially-configured dual-spacecraft formation in a deep space environment. In these applications, Γ_{GG} is nearly constant during the short time periods associated with scientific observations.

The complete dynamics model for the dual-spacecraft formation alignment GN&C will also include the rigid body attitude equations of motion[19], for both Detector spacecraft and Optics spacecraft, as given in the general form of Eq. (12) and Eq. (13). This results in a nine DoF state model which is coupled through optical measurements of relative position, when considering sensor locations not coincident with respective spacecraft center of mass, as given in Eq. (5) and Eq. (6).

$$\dot{q} = \tfrac{1}{2}\widetilde{\Omega} q \tag{12}$$

$$\dot{\vec{\omega}} = I_S{}^{-1}(\vec{\omega} \times I_S\,\vec{\omega}) + \vec{T} \tag{13}$$

Measurement models for GN&C design may also include those for rate gyros, Eq. (14), and accelerometers, Eq. (15) [10].

$$\dot{\vec{\theta}} = \vec{\omega}^m - \vec{b}_\omega + \vec{\nu}_\omega \tag{14}$$

$$\begin{aligned}\ddot{\vec{\delta}}^m &= \left([I] - \tilde{r}_A I_S{}^{-1}\tilde{r}_T\, m_S\right)\vec{u}_{F_{T_0}} + \left([I] - \tilde{r}_A I_S{}^{-1}\tilde{r}_T\, m_S\right)\overrightarrow{\delta u}_{F_T} \\ &+ \left([I] - \tilde{r}_A I_S{}^{-1}\tilde{r}_E m_S\right)\vec{u}_{F_E} + \vec{b}_A + \vec{\nu}_A\end{aligned} \tag{15}$$

The complete framework for the VT GN&C design includes dynamics models, Eq. (8)-(13), measurement models for optical sensors, Eq. (1)-(7), and inertial sensors, Eq. (14)-(15).

One should note, when using the quaternion kinematics of the form in (12) for model-based filter design, care should be taken to avoid potential numerical issues due to the implicit normalization constraint of the unit quaternions used for attitude representations. One 3-parameter representation used to avoid this constraint is known as Modified Rodriguez Parameters, considered by Karlgaard[20] and Crassidis[21.] One example of a quaternion based filter is the Multiplicative Extended Kalman Filter (MEKF)[22,23,24]. The MEKF addresses the quaternion constraint issue by estimation of a 3-parameter small angle attitude state and the use of a multiplicative quaternion residual. A reset operation is used to preserve the unit norm of the reference quaternion. The MEKF is a practical solution when using quaternion output star trackers, as well as having other computation and conceptual advantages, as discussed in Markley[23,24].

GN&C Architectures for VT PFF

The GN&C system for the VT PFF is an example of a distributed spacecraft system involving control of two spacecraft that function together to form a single scientific measurement system. Depending on the placement of PFF sensors and actuators significant spacecraft dynamic coupling could result in the GN&C system, as shown in the measurement and dynamics models provided in the previous section. Two different approaches to GN&C architecture design illustrate this coupling.

The Leader/Follower architecture, shown in Figure 4, provides a representative PFF sensor and actuator placement as one possible GN&C configuration. The Detector spacecraft is the actively controlled element for the VT PFF, the Optics spacecraft (Leader) would perform only 3-axis attitude determination and control, and the Detector spacecraft (Follower) would perform 3-axis attitude and 3-axis relative position control. A full-state estimator (nine DoF) that processes all measurements serves to consolidate the relative state estimation onboard the Detector spacecraft. The Detector spacecraft requires thrusters for relative position control so it is natural to also use thrusters for attitude control in a 6-axis configuration, thus avoiding the need for reaction wheels (RW) for attitude control. Attitude control for the Optics spacecraft could optionally use RW or thrusters. A set of three-axis thrusters would anyway be included for momentum unloading when using the RW, since magnetic torqueing is not available in deep-space orbit applications.

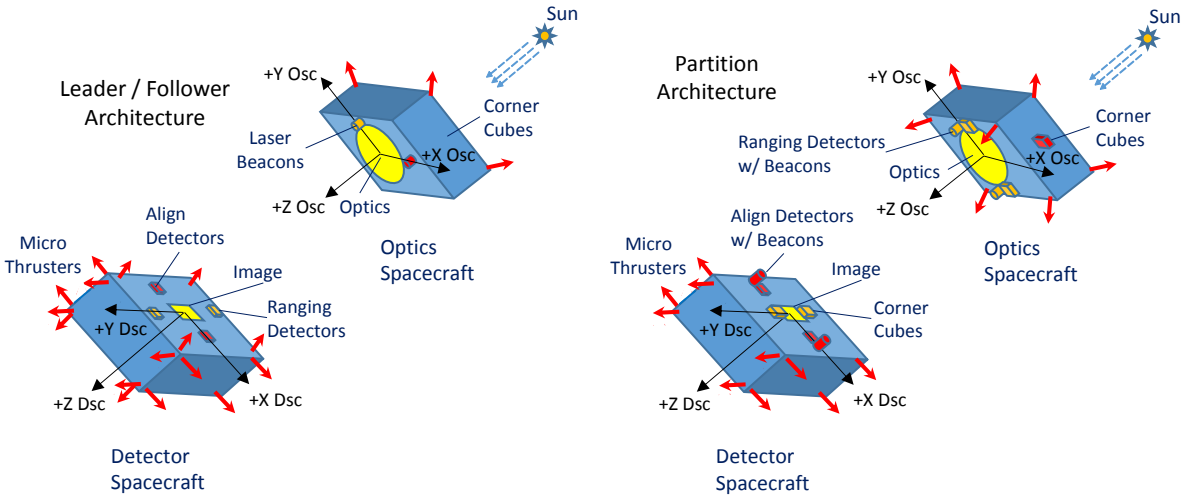

Figure 4. Representative GN&C Architectures for the VT

This leader/follower architecture has two possible deficiencies. First, due to attitude coupling in the optical metrology measurements, a communication link is required to send attitude data from Optics spacecraft to Detector spacecraft for use in the full-state navigation filter. This may suffer from possible uncertain transmission delay and timing synchronization across the inter-spacecraft communication link. Second, the thruster system for the Detector spacecraft is required to perform simultaneous 6-axis control. Providing a feasible thruster configuration that sufficiently decouples all axes for precision full-state control may be difficult. The leader/follower architecture shown in Figure 4 includes a set of 24 thrusters in a 6-axis decoupled configuration.

An alternate partitioned architecture that addresses these concerns is also shown in Figure 4. In this case, the control and estimation is partitioned among the two spacecraft and the optical sensors are located to avoid the multi-platform attitude coupling in the measurement process. The Optics spacecraft controls the 3-axis attitude and relative range, and the Detector spacecraft controls the 3-axis attitude and transverse alignment only. The decoupling of laser alignment measurements on

the Detector spacecraft and laser ranging measurements on the Optics spacecraft is achieved by proper placement of respective optical elements. First, laser beacons for both alignment and ranging measurements are pointed to corner cube reflectors mounted on the opposing spacecraft. The return beams are acquired at collocated detectors, respectively. The attitude dependency in the return beam, arising from the $\tilde{P}_{LB}$ term in Eq. (5), is eliminated since the elements of Φ in Eq. (5) are equal to 0 when using corner cubes. The remaining attitude dependent coupling between spacecraft in Eq. (5) is eliminated by locating the corner cubes for laser alignment return (on the Optics spacecraft) in the x-y plane, and the corner cubes for the laser ranging return (on the Detector spacecraft) along the z axis.

CASE STUDY: GN&C DESIGN FOR A HELIOPHYSICS MISSION

The model-based framework for GN&C design, as developed in this work, was applied to an example problem to illustrate the performance trades inherent in dual-spacecraft PFF for VT applications. The dual-spacecraft PFF technology has many applications in various scientific investigations that require a long baseline VT, such as in high energy imaging[1-4]. One such proposed heliophysics VT mission uses a photon sieve for high resolution solar imaging[25]. The photon sieve is a type of diffractive optics for producing narrowband focused images. Achieving high resolution diffraction-limited imaging in high energy wavelengths requires long baselines, large precision manufactured optics, and precise alignment and range control stability[25]. The GN&C requirements representative of a milli-arc-sec level photon sieve application are given in Table 1. These precise requirements consequently place demanding specifications on GN&C architectures and sensors, particularly on optical metrology[16] needed for precise alignment sensing. The specifications for the compliment of sensor and actuators used in this study are also provided in Table 1. These values represent the approximate levels needed to achieve the given science requirements.

Table 1. Photon Sieve VT Alignment Requirements and Component Specifications

Parameter	Requirement (3σ)
Image Smear	6 microns
Depth of Field	1 mm
spacecraft separation	200 m
Pointing Stability (Optics spacecraft)	5 milli-arc-sec (Sun) 10 arc-sec (roll)
Pointing Stability (Detector spacecraft)	10 arc-sec

Component	Specification (3σ)
Laser Alignment	30 microns
Laser Ranging	0.5 cm
Microthruster	5 μN-sec (min Impulse)
Fine Sun Sensor	30 milli-arc-sec
Star Tracker	6 arc-sec (transverse) 30 arc-sec (boresight)

GN&C Mode Design

The case study scenario includes transitioning the PFF system through three representative GN&C modes (Acquisition, Coarse-Align, and Fine-Align), as shown in Figure 5. This is a staged approach to acquire the laser beacons within the respective detector elements of the precision alignment configuration. Acquisition mode uses radio-based range and bearing measurements for relative navigation, providing a large relative range envelope for initial operation. The end state of this initial acquisition is alignment of the two spacecraft, placing the Optics spacecraft with the field of view of a camera-based imager mounted on the Detector spacecraft for relative navigation. This imager provides alignment precision of less than 3 millimeters in the Coarse Align mode. Precision alignment (< 6 microns) is achieved in the Fine Align mode using the laser alignment sensor (detector size = 1 cm). The sensor compliment and measurement error for each PFF mode is given in Table 2. The measurement error statistics were also used to initialize the states and error

covariance for navigation filter. This mode design illustrates a practical approach for achieving fine alignment from an initial acquisition using radio-based ranging navigation.

Figure 5 shows the result of a single leader/follower case, illustrating the PFF cross-range alignment performance in each GN&C mode. The simulation is started in the Acquisition mode with sun pointing attitude and a 20 m separation along VT axis and 4 m transverse error. The initial velocity in each axis was set to 2 cm/sec. The control response (not shown) converges to a 200 m separation command after about two hours. During this time the navigation filter converges to less than 0.5 m. After three hours the PFF mode is set to Coarse Align using an alignment camera to track two beacons mounted on the Optics spacecraft (beacons separated by 2 m on a target structure). This provides a measure of range and bearing that results in cross-range navigation error convergence to mm level after one hour. After three hours in Coarse Align mode the PFF system is set to Fine Align mode and the laser ranging and alignment sensors are used to converge the filter solution to less than 6 microns (3σ) transverse error. The navigation filter state and covariance are initialized using radio range (60 cm (3s) and bearing (30 deg (3σ)) measurements. The filter error covariance bound (3σ), shown in dashed lines, illustrates reasonable filter convergence to steady-state during each mode transition.

Table 2. Case Study: Sensor Compliment and Measurement Errors (3σ) for PFF Modes

GN&C Hardware	Acquisition	Coarse Align	Fine Align
Radio Ranging	60 cm		
Radio Bearing	30 deg		
Alignment Camera		50 arc-sec	
Laser Ranging			1 cm
Laser Alignment			30 μm
Star Tracker	6 arc-sec (transverse) 30 arc-sec (boresight)	6 arc-sec (transverse) 30 arc-sec (boresight)	6 arc-sec (transverse) 30 arc-sec (boresight)
Fine Sun Sensor			10 milli-arc-sec

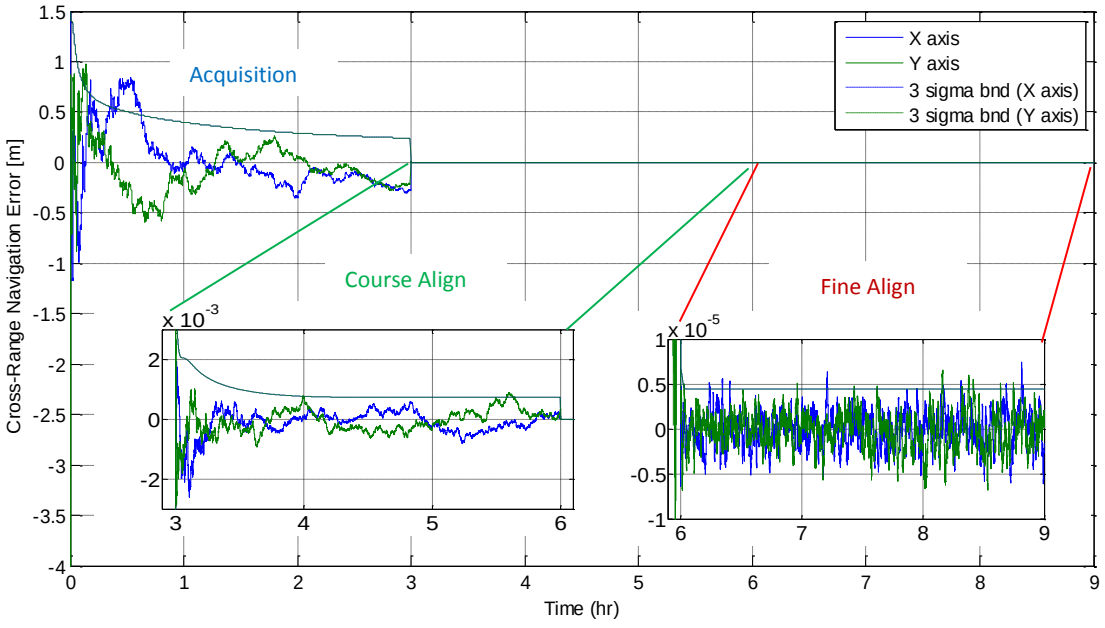

Figure 5. Leader/Follower Case: Separation through Stabilization at 200m baseline

Monte Carlo Study of GN&C Architectures

The performance of the Leader/Follower and Partition GN&C architectures, described in the previous section, were analyzed in a high-fidelity Matlab/Simulink simulation with the complete nine DoF dynamics. The PFF scenario, as represented by a single case in Figure 5, was simulated in a Monte Carlo (MC) analysis for each alternative architecture. MC runs include variations in mass properties (given in Table 3) as well as initial navigation state/covariance errors, truth model initial condition error, and sensor model errors, all consistent with the measurement errors shown in Table 2 for the Acquisition mode. The state estimation was implemented as an Extended Kalman Filter using a continuous form for state propagation and discrete measurement updates[26]. Measurement updates were performed sequentially to avoid numerical issues associated with computation of large matrix inverses. Separate PID controllers are used for attitude and relative position states. While other choices of GN&C design algorithms are possible for this application, the standard methods used for this study are easy to implement and have good computational characteristics. They provide a good baseline approach for comparison of different PFF architectures. All measurement and actuator models include first-order Markov processes to represent systematic errors within the control bandwidth, in addition to random noise at the levels provided in Table 1. This modeling approach facilitates assessment of the GN&C system's performance robustness in the presence of unmodeled errors. The GN&C system operates at a 10 Hz update for both navigation filter and control actuation.

Table 3. Case Study: Mass Properties and Monte Carlo Variations

Parameter	Nominal Value (kg)	Variation (3σ)
Optics spacecraft Mass	200 kg	+/- 10%
Detector spacecraft Mass	400 kg	+/- 10%
Optics spacecraft Radius of Gyration	1 m	+/- 10%
Detector spacecraft Radius of Gyration	1 m	+/- 10%

Figure 6 shows lateral alignment error results from 400 cases, along with 95% confidence ellipses, for both GN&C architectures (Leader/Follower (blue), Partition (red)). These results are an ensemble average taken at the end of a 9 hour scenario after transitioning though each PFF mode as shown in Figure 5. MC results indicate that errors in transverse axes are uncorrelated, which is expected due to lack of significant cross-axes coupling in state dynamics and measurement models for these architectures. Results indicate that transverse alignment errors are somewhat better for the Partition architecture. Decoupling of the laser alignment measurement from the Optics spacecraft attitude, by the proper positioning the corner cube reflectors, results in improved transverse alignment observability in the Partition architecture. The Partition architecture performance meets the alignment requirements for the Photon Sieve application as listed in Table 1, illustrating the improvement obtained from model-based estimation over unfiltered laser alignment measurements. Using a Kalman filter framework the error is reduced by approximately a factor of five over the baseline position sensor measurements in this case.

Figure 6 also shows the total impulse required for PFF over a five year mission for both architectures. Total impulse required to maintain alignment is significantly higher for the Leader/Follower architecture. The partitioned GN&C architecture requires about 35% less total impulse because the Optics spacecraft, which performs range control, is half of the mass of Detector spacecraft. Performance comparison of these two alternative PFF architectures demonstrates the

system trades that result from the measurement/state coupling and control actuator partitioning inherent in the dual-spacecraft PFF GN&C system presented in this paper.

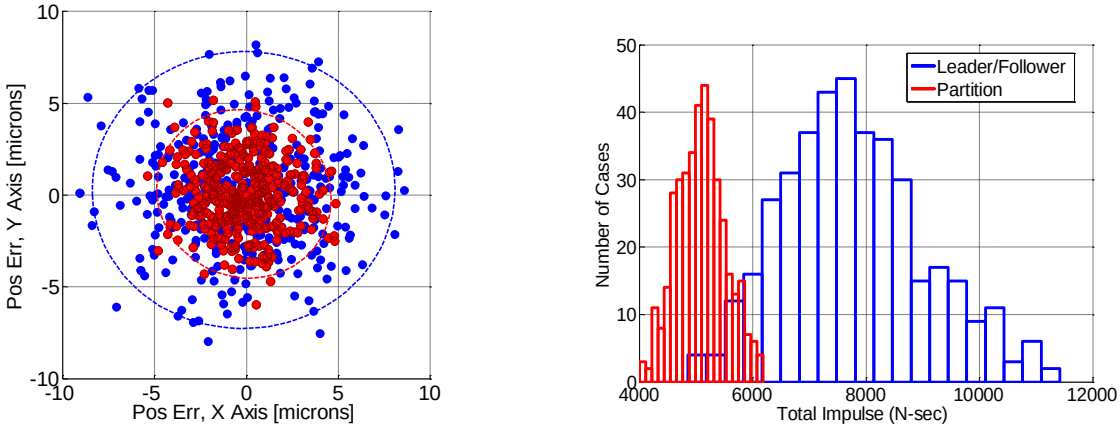

Figure 6. Performance Results of Two Representative GN&C Architectures for the VT

CONCLUSION

A general framework for dual-spacecraft PFF GN&C architecture design has been developed with specific application to VT missions. The development includes models for dynamics and measurement processes for systems that employ non-collocated sensors and actuators, including laser-based alignment and ranging systems, optical imaging sensors, and inertial measurement units (IMU), as well as microthrusters. These models are found to be applicable to short baseline VT applications of near term interest (spacecraft separation range: 50 – 500m). Their usefulness would be reduced as the spacecraft separation increases relative to size of each spacecraft. A GN&C performance assessment is given for a representative Heliophysics PFF imaging mission concept with 200-400 kg satellites at 200 m separation. The study results reveal how data from relative position sensors can be employed in a Kalman filter framework to significantly improve alignment estimation performance over the baseline position sensor measurements. The case study also provides a comparison of two different GN&C formation flying architectures, illustrating the performance trades inherent in the choice of system architecture for PFF in the VT application.

ACKNOWLEDGMENTS

The authors would like to acknowledge Joe Davila and Doug Rubin for their support, technical oversight, and assistance in understanding the scientific objectives of the Photon Sieve VT concept, and Michael Johnson for his support of the IRAD effort to accomplish this work.

NOTATION

$\vec{b}_A$	Accelerometer Measurement Bias
$\vec{b}_\omega$	Gyro Measurement Bias
m_S	Spacecraft Mass
q	Attitude Quaternion
$\vec{r}_{iD}$	Detector Spacecraft Position relative to ith Central Body
$\vec{r}_A$	Accelerometer Location Vector relative to Mass Center
$\vec{r}_E$	Environmental Disturbance Action Point Location Vector relative to Mass Center
$\vec{r}_T$	Thruster Location Vector relative to Mass Center

$\vec{u}_{\mathrm{F_E}}$	Environmental Disturbance Specific Force on Follower Spacecraft
$\vec{u}_{\mathrm{F_{T_0}}}$	Nominal Thruster Specific Forces for Control of Follower Spacecraft
$\vec{u}_R$	Leader/Follower Total Differential Specific Force
$\vec{u}_{thrust,D}$	Thruster Specific Force on Detector Spacecraft
$\vec{u}_{thrust,O}$	Thruster Specific Force on Optics Spacecraft
$\bar{x}$	Relative Spacecraft Position
$[I]$	Identity Matrix (3x3)
I_S	Spacecraft Inertia
$\vec{P}_B$	Laser beacon Position relative to Optics spacecraft Mass Center
$\vec{P}_C$	Camera-based sensor Position relative to Detector spacecraft Mass Center
$\vec{P}_D$	Detector Assembly Position relative to Detector spacecraft Mass Center
$\vec{P}_O$	Optics Assembly Position relative to Optics spacecraft Mass Center
$\vec{P}_{CO}$	Camera-based sensor Position relative to Optics spacecraft Mass Center
$\vec{P}_{DO}$	Detector Assembly Position relative to Optics spacecraft Mass Center
$\vec{T}$	Spacecraft External Torque
$\ddot{\vec{\delta}}^m$	Spacecraft Measured Acceleration
$\vec{v}_\omega$	Gyro Measurement Noise
$\vec{v}_A$	Accelerometer Measurement Noise
μ_i	Gravitational Constant for ith Central Body
$\vec{\theta}$	Attitude Vector
θ_O	Optics spacecraft to Astrometric Sensor boresight alignment angles
θ_G	Guide Star to Astrometric Sensor boresight alignment angles
θ_{δ_R}	Relative Spacecraft Alignment Angles
$\vec{\omega}$	Angular Rate Vector
$\vec{\omega}^m$	Measured Angular Rate Vector
$\Delta\vec{f}_{solar}$	Differential Solar Pressure Specific Force
$\Delta\vec{f}_{pert}$	Differential Gravitational Perturbations
$\widetilde{\Omega}$	Angular Velocity four-dimensional skew-symmetric Matrix

REFERENCES

[1]G. K. Skinner, Z. Arzoumanian, W. C. Cash et al., "The milli-arc-second structure imager (MASSIM): a new concept for a high angular resolution x-ray telescope," in *Space Telescopes and Instrumentation 2008: Ultraviolet to Gamma Ray*, vol. 7011of *Proceedings of SPIE*, Marseille, France, June 2008.

[2]G. K. Skinner, B. R. Dennis, J. F. Krizmanic, E. P. Kontar, "Science Enabled by High Precision Inertial Formation Flying", International Journal of Space Science and Engineering, Vol. 1, No. 4, 2013, pp. 331-348

[3]Cash, W., Oakley, P., Turnbull, M., Glassman, T., Lo, A., Polidan, R., Kilston, S., Noecker, C., "The New Worlds Observer: scientific and technical advantages of external occulters", SPIE, 7010, 1Q, 2008.

[4]Cash, W. "Detection of Earth-like planets around nearby stars using a petal-shaped occulter." *Nature*, 442, no. 7098, 2006, pp. 51-53.

[5]Cash, W., Kendrick, S., Noecker, C., Bally, J., DeMarines, J., Green, J., Oakley, P., Shipley, A., Benson, S., Oleson, S., Folta, D., "The New Worlds Observer: the astrophysics strategic mission concept study", *SPIE Optical Engineering+ Applications* (pp. 743606-743606). International Society for Optics and Photonics, August 2009

[6]Deccia, C.M.A, "Analysis of the Sun-Earth Lagrangian environment for the New Worlds Observer (NWO)", Master's Thesis, Dept. of Aerospace Engineering, Delft University of Technology, Delft, Netherlands, June 6, 2017

[7]Starin, S., "Formation Flying Mission Concept for Observing Solar Eruptive Events," *International Conference on Spacecraft Formation Flying Missions and Technologies*, May 2011.

[8]Lamy, P., Damé, L., Vivès, S., Zhukov, A., "ASPIICS: a giant coronagraph for the ESA/PROBA-3 Formation Flying Mission", *Space Telescopes and Instrumentation 2010: Optical, Infrared, and Millimeter Wave* (Vol. 7731, p. 773118). International Society for Optics and Photonics, 2010.

[9]Dennis, B. R., Skinner, G. K., Li, M. J., Shih, A. Y. "Very High-Resolution Solar X-Ray Imaging Using Diffractive Optics," Solar Physics, Vol. 279, 2012, 573-588

[10]Calhoun, P., Shah, N., "Covariance Analysis of Astrometric Alignment Estimation Architectures for Precision Dual Spacecraft Formation Flying." *AIAA Guidance, Navigation, and Control Conference*.

[11]Luquette, R. J. and Sanner, R.M., "Spacecraft Formation Control: Managing Line-of-Sight Drift Based on the Dynamics of Relative Motion," *Formation Flying Symposium*, April 2008.

[12]Luquette, R. J. and Sanner, R. M., "Linear State-Space Representation of the Dynamics of Relative Motion, Based on Restricted Three Body Dynamics," *AIAA Guidance and Control Conference*, August 2004, Paper No. AIAA-2004-4783

[13]Luquette, R. J. and Leitner, J. and Gendreau, K. C. and Sanner, R. M., "Formation Control for the MAXIM Mission," *2nd International Symposium on Formation Flying Mission & Technolo8gies*, September 2004.

[14] Luquette, R. J., "Nonlinear Control Design Techniques for Precision Formation Flying at Lagrange Points," Ph.D. Dissertation, Department of Aerospace Engineering, University of Maryland, College Park, MD, December 2006.

[15] Novo-Gradac. A., "Alignment Requirements for Distributed Telescope", *Unpublished White Paper*, January 2017.

[16] Novo-Gradac. A., "Relative Position Sensing System for a Precision Formation Flying Space Telescope," *9th International Workshop on Satellite Constellations and Formation Flying*, Boulder, Co., June 19-21, 2017.

[17] Howard, R.T., Heaton, A. F., Pinson, R. M., Carrington, C. L., Lee, J. E., Bryan, T. C., ... & Johnson, J. E. (2008, January), „The advanced video guidance sensor: orbital express and the next generation". In M. S. El-Genk (Ed.), *AIP Conference Proceedings* (Vol. 969, No. 1, pp. 717-724). AIP.

[18] Bryan, T. C., Howard, R., Johnson, J. E., Lee, J. E., Murphy, L. and Spencer, S. H., "Next Generation Advanced Video Guidance Sensor," *2008 IEEE Aerospace Conference*, Big Sky, MT, 2008, pp. 1-8

[19] Wertz, J.R., *Spacecraft Determination and Control*, Kluwer Academic Publishers, Dordrecht, Netherlands, 1978.

[20] Karlgaard, C.D., Schaub., H. "Nonsingular Attitude Filtering Using Modified Rodrigues Parameters", The Journal of the Astronautical Sciences, 2009, 57:4, 777-791.

[21] Crassidis, J.L., Markley, F. L., "Attitude estimation using modified Rodrigues parameters", *Proceedings of the Flight Mechanics/Estimation Theory Symposium*, (NASA/CP-1996-3333), NASA-Goddard Space Flight Center, Greenbelt, Md., pp. 71-83, 1996.

[22] Lefferts, E. J., Markley, F. L., and Shuster, M. D.,"Kalman Filtering for Spacecraft Attitude Estimation", Journal of Guidance, Control, and Dynamics, Vol. 5, No. 5, 1982, pp. 417-429.

[23] Markley, F. L., "Attitude Error Representations for Kalman Filtering", Journal of Guidance, Control, and Dynamics, Vol. 63, No. 2, 2003, pp. 311–317

[24] Markley, F. L., "Multiplicative vs. additive filtering for spacecraft attitude determination", Proceedings of the Sixth Conference on Dynamics and Control of Systems and Structures in Space (DCSSS), vol. D22, Riomaggiore, Italy, July 2004.

[25] Davila, J. M., High-resolution solar imaging with a photon sieve. Proc. SPIE 8148, Solar Physics and Space Weather Instrumentation IV, 81480O, (October 07, 2011)

[26] Gelb, A. (ed.), *Applied Optimal Estimation*, The MIT Press, Cambridge, MA, 1974